ELSEVIER

Soil & Tillage Research 47 (1998) 133–143

Soil & Tillage Research

Spatio-temporal dynamics of water and heat in a field soil

B.P. Mohanty*, P.J. Shouse, M.T. van Genuchten

U.S. Salinity Laboratory, 450 W. Big Springs Road, Riverside, CA 92507, USA

Abstract

Soil water content (Θ) and soil temperature (T) near the land–atmosphere boundary interactively govern upward and downward fluxes of water and energy. To date few if any comprehensive studies have examined the spatio-temporal variability and interactive relationships between Θ and T at the field-scale. This information is required for field-scale modeling of non-isothermal water, heat, and chemical transport in soil. As well, it may prove useful for modeling the near-surface atmosphere component of General Circulation Models and addressing related scale issues. The objectives of this study were to (i) simultaneously monitor, with high temporal resolution, the soil water content and soil temperature at a large number of spatial locations and depths in a field under different soil moisture conditions, and (ii) study the spatio-temporal variability and functional correlation of the two state variables Θ and T at the field-scale. Soil water content and soil temperature measurements were made at 20 min intervals at 49 regularly-spaced (1.0 m) locations and at 3 depths along two transects in a bare field in Riverside, California. Measurements were made for a period of 45 days during different irrigation events. More than 150 TDR probes and 150 thermocouples were used in conjunction with 25 multiplexers and several data loggers for automatic monitoring. Correlation analysis of the data revealed a diurnal spatio-temporal hysteresis in the mean and variance of T during dry and wet days. Corresponding Θ-values did not exhibit much spatio-temporal hysteresis, although they had a tendency to cluster across time at different depths.

Keywords: Water flow monitoring; Heat flow monitoring; Spatio-temporal variability

1. Introduction

Soil moisture (Θ) and soil temperature (T) in the shallow subsoil play a pivotal role in the global water and energy balance. The spatial and temporal dynamics of water and energy transport across the soil–atmosphere boundary layer in relation to near-surface hydrology and thermodynamics, land use, and climate change is still poorly understood, thus seriously limiting the capabilities and accuracy of current meso-scale hydrologic and General Circulation models (GCMs). Understanding the spatio-temporal variability of Θ and T at different scales in space (plot, field, watershed, region, continent) and time (day, month, season, decade, century) is an increasingly critical issue in the hydrological sciences. Quantifying the space-time dynamics of water and heat requires well-designed experiments of water and heat flow in soil at a hierarchy of space and time scales, in conjunction with appropriate modeling efforts. Such an approach is especially promising now that powerful remote sensing techniques (e.g., passive microwave radio-

*Corresponding author.

0167-1987/98/$19.00
PII S0167-1987(98)00084-1

meter, gamma ray radiometer, thematic mapper) are becoming available to obtain large-scale soil water content and heat flux measurements, while simultaneously a variety of in situ measurement techniques (e.g., time or frequency domain reflectrometry, neutron probe or thermocouple procedures) exist to also obtain point-scale Θ and/or T data.

At the field or larger scale, Θ and T are influenced by several soil-physical, topographical, biological, and management factors, as well as by such atmospheric state variables as diurnally and seasonally variable solar radiation, wind speed, humidity, latent heat, and sensible heat. Soil-associated properties generally exhibit inherently strong spatial variations, while atmospheric variables are mostly subject to large temporal variations. Hence, soil water contents and soil temperatures constantly undergo spatio-temporal variations. Long-term larger-scale hydrologic studies can often adopt at most a daily sampling scheme for Θ and T when using conventional labor-intensive approaches such as those involving gravimetric sampling, neutron probe measurements, and other in situ soil moisture or temperature sampling techniques [e.g., recent hydrologic experiments by NASA and USDA as well as others such as those by Hills et al., 1991; Parlange et al., 1993; Shouse et al., 1992, 1994; Mohanty et al., 1997; Capehart and Carlson, 1997; and SGP'97 (http://hydrolab.arsusda.gov/~tjackson/)]. Remote sensing approaches are often also limited to daily-measurements in view of the high operational costs involved [e.g., cooperative hydrology experiments of NASA, USDA, and others including: Washita'92 (Jackson et al., 1995); Washita'94 (Jackson, 1997); Capehart and Carlson, 1997; and SGP'97 (http://hydrolab.arsusda.gov/~tjackson/)].

In studies where short-term fluctuations in water or heat flow are more important, small plots or lysimeters with few monitoring points are generally used for high-resolution Θ and T measurements [e.g., Staple, 1965, 1969; Shouse et al., 1992; Radke et al., 1993; Evett et al., 1994; Mohanty et al., 1995; Noborio et al., 1996]. These and other studies [e.g., Georgakakos, 1996] show that space-extensive experiments often overlook important information related to the temporal dynamics of water and heat across the diurnal cycle. On the other hand, time-intensive Θ and T monitoring schemes often do not accurately assess detailed spatial variability due to heterogeneity in soil properties, vegetation characteristics, climate condition, or other extrinsic variables across the landscape.

Whereas a number of independent spatial and temporal variability studies of either Θ or T have been made before, few if any studies have addressed the spatio-temporal variability and interactive relationships of these two state variables at the field or higher scales. Such studies at different scales are needed to better understand and quantify the dynamics of water and heat in GCMs [e.g., Bell et al., 1980], especially when collocated measurement of Θ and T are made in large land areas with small time steps. The objectives of this study were to: (i) simultaneously monitor Θ and T with high temporal resolution under different soil moisture conditions in an irrigated field, and (ii) study the spatio-temporal variability and functional correlation of the two state variables (Θ and T) at the field-scale.

2. Field experiment

During the fall of 1995 (October 25–December 10) we conducted a large water and heat transport field experiment in the shallow subsurface along two orthogonal transects comprising 49 regularly spaced (1.0 m) sites near the University of California agricultural experimental station in Riverside, California. The general climate of this area is arid with large diurnal variations in temperature. Soil at the field site was Arlington fine sandy loam (coarse-loamy, mixed, thermic, Haplic Durixeralf). Our experimental field was flat and kept bare during the study. Herbicide was applied to prevent any weed growth near the monitoring locations. Trenches with 49 narrow ports were excavated along the transects as shown in Fig. 1. Three sets of TDR probes (Campbell Scientific, Logan, Utah) for measuring soil water content, and copper–constantan thermocouples for measuring soil temperature were inserted horizontally into the walls of each port at the depths of 2, 7, and 12 cm below the soil surface. The probes were connected to 20 TDR multiplexers (5DMX50), and 5 thermocouple multiplexers (AM416), several data loggers (CR10, 21x, Campbell Scientific, Logan, Utah), and 2 TDR cable testers (1502B, Tektronix, Beaverton, Oregon). Multiplexers were housed at several locations in the soil

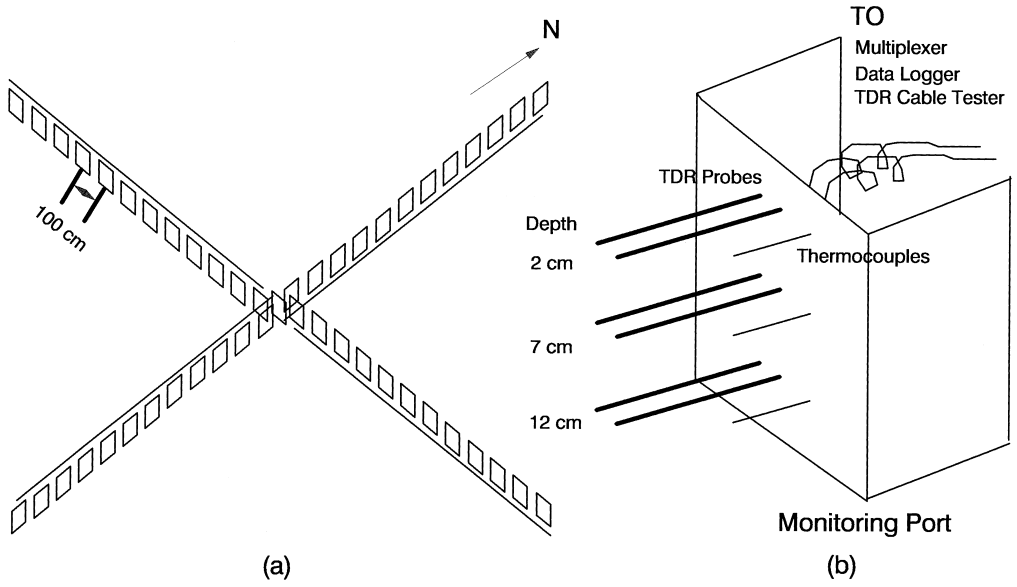

Fig. 1. (a) Experimental layout showing 49 monitoring ports (1 m apart) organized along two orthogonal transects (n-s and e-w), (b) A single port equipped with TDR probes and thermocouples at different depths for measuring Θ and T, respectively.

using water- and temperature-resistant boxes, and connected serially to a central monitoring location. The central monitoring and distribution unit was connected to a source at 110 V. After installation of all necessary hardware, trenches were carefully backfilled to the original soil bulk density. The soil surface was later chiseled to remove any surface undulation or microtopography and to open any clogged pore-spaces.

The field was equipped with a sprinkler irrigation system having several laterals and outlet ports. Catch cans near the monitoring ports were used to measure water input and distributions. A weather station adjacent to the experimental plot was used to monitor diurnal variations of near-surface (20 and 80 cm above the soil surface) air temperature, relative humidity, wind speed, net radiation, and other atmospheric parameters. Soil water content and soil temperature at each location and depth were measured at between 20–60 min intervals. The automatic monitoring system was programmed to follow a cyclic routine with regular intervals for different sites and depths. We downloaded the data every third day from the data loggers to a portable computer. The measurements continued for 45 days (Julian day 300–345) under several dry and wet spells induced with the sprinkler system. No natural precipitation occurred at the field site during our experiment. The automated monitoring system worked nearly flawlessly for most of the experiment, except for days when some of the data were lost because of temporary failure of the system.

3. Results and discussion

The experiment yielded a comprehensive set of Θ and T measurement of high spatial and temporal resolution. This paper summarizes results obtained during Julian days 328–338 covering both dry and wet soil moisture conditions. In the following sections we will sequentially discuss the spatial variability, temporal variability, and spatio-temporal variability of the Θ and T data.

3.1. Spatial distribution of Θ and T

Figs. 2 and 3 show measured Θ and T values at three depths (2, 7, and 12 cm) across the east-west (e-w)

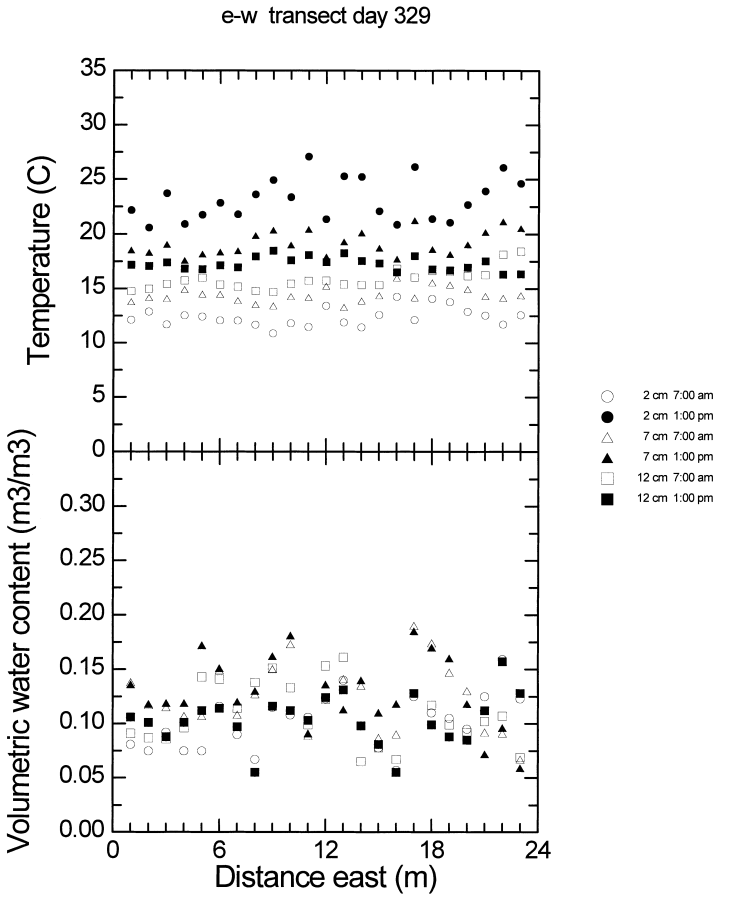

Fig. 2. Spatial variability of volumetric soil water content (Θ) and soil temperature (T) at different depths and times across e-w transect on a pre-irrigation day (day 329).

transect at two discrete times: 7:00 am and 1:00 pm. These two times roughly coincided with the diurnal minimum and maximum surface soil temperature (i.e., at 2 cm depth) at several monitoring locations. Although we could not find a clear maximum or minimum soil moisture content across the diurnal cycle, we present the Θ data at 7:00 am and 1:00 pm only for comparison purposes. Late in the mornings of day 334 and day 335 two light irrigations were applied. Because of staggered sprinkler (rainfall) pattern, the irrigation rate on day 334 varied spatially between 3.88–7.57 mm across the field with a mean of 5.3 mm and variance 1 mm^2. On day 335, the irrigation rate varied between 1.08–2.78 mm with a spatial mean 1.8 mm and variance 0.2 mm^2. Data are presented here for two days, a pre-irrigation day (329) and an irrigation day (334), to reveal differences in the spatial patterns of Θ and T under different soil water conditions. Weather conditions for these two days were quite similar. Figs. 2 and 3 show that the mean and diurnal scatter of T for the three depths across the e-w transect decreased somewhat after the irrigation. The mean T across the three depths of the n-s transect also decreased after the irrigation but not its range (results not shown here). At most monitoring sites T followed the expected pattern versus depth: $T_{2\ \mathrm{cm,\ 1\ pm}} > T_{7\ \mathrm{cm,\ 1\ pm}} > T_{12\ \mathrm{cm,\ 1\ pm}} > T_{12\ \mathrm{cm,\ 7\ am}} > T_{7\ \mathrm{cm,\ 7\ am}} > T_{2\ \mathrm{cm,\ 7\ am}}$. The presence of differing diurnal ranges at different sites in the field, however, indicated differential rates of heating and

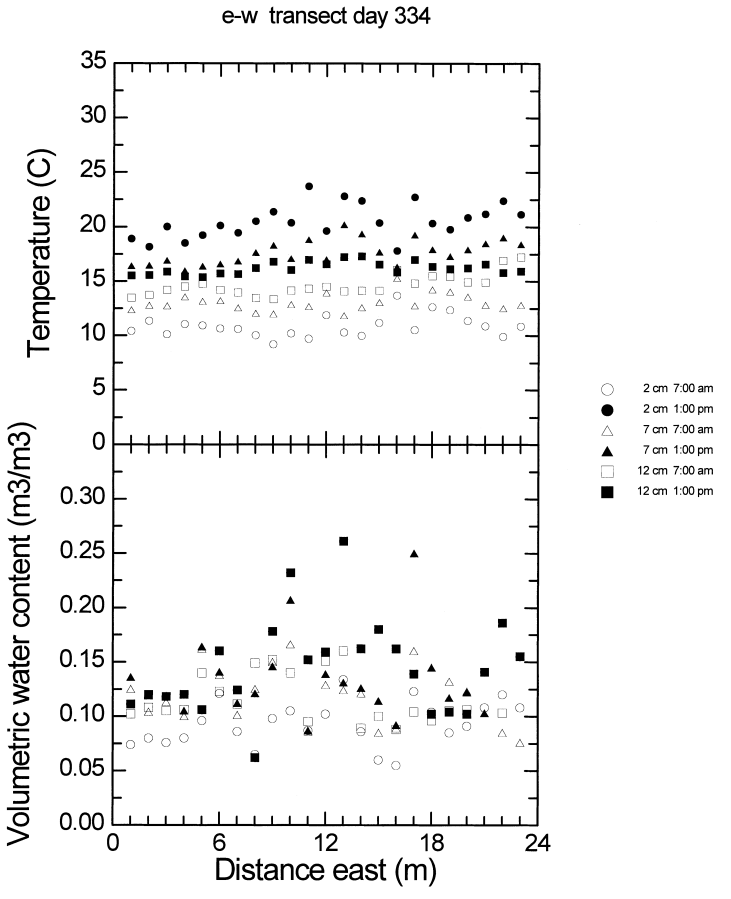

Fig. 3. Spatial variability of volumetric soil water content (Θ) and soil temperature (T) at different depths and times across an e-w transect on an irrigation day (day 334). Irrigation occurred between 10:00 am and 12:00 noon.

cooling across the field. Also, the temperature at three sites (east 16, 22, and 23) for T during solar noon (1:00 pm) was found to be lower than T at 7:00 am at the 12 cm depth for all soil moisture scenarios. On day 334 we generally found larger diurnal changes in T at the wetter sites (e.g., east 10 and 17) as compared to the drier sites (e.g., east 2, 3, 18, and 19), although some exceptions did exist (e.g., east 12). These patterns can be explained by the presence of different heating and cooling caused by the Θ-dependent soil thermal properties.

The soil water contents across the e-w or n-s transects did not exhibit any specific spatial pattern. However, the data did show several interesting features. For example, $\Theta_{7\ \mathrm{cm}}$ on a relatively dry day (329) along the e-w transect was generally higher than $\Theta_{2\ \mathrm{cm}}$ and $\Theta_{12\ \mathrm{cm}}$ indicating both upward and downward moisture gradients away from the 7 cm depth. By comparison, $\Theta_{12\ \mathrm{cm}}$ along the n-s transect was generally higher than $\Theta_{2\ \mathrm{cm}}$ and $\Theta_{7\ \mathrm{cm}}$. Also, shortly after the irrigation event on day 334, $\Theta_{2\ \mathrm{cm}}$ and $\Theta_{12\ \mathrm{cm}}$ on the e-w transect were similar and higher than $\Theta_{7\ \mathrm{cm}}$, while $\Theta_{2\ \mathrm{cm}}$ on the n-s transect (not shown here) was generally higher than $\Theta_{7\ \mathrm{cm}}$ and $\Theta_{12\ \mathrm{cm}}$. Specific changes in Θ between morning (7:00 am) and afternoon (1:00 pm) at any depth varied from site to site reflecting some spatial variability in the soil hydraulic properties and their temperature dependence across the field, and likely also some variability in irrigation water input.

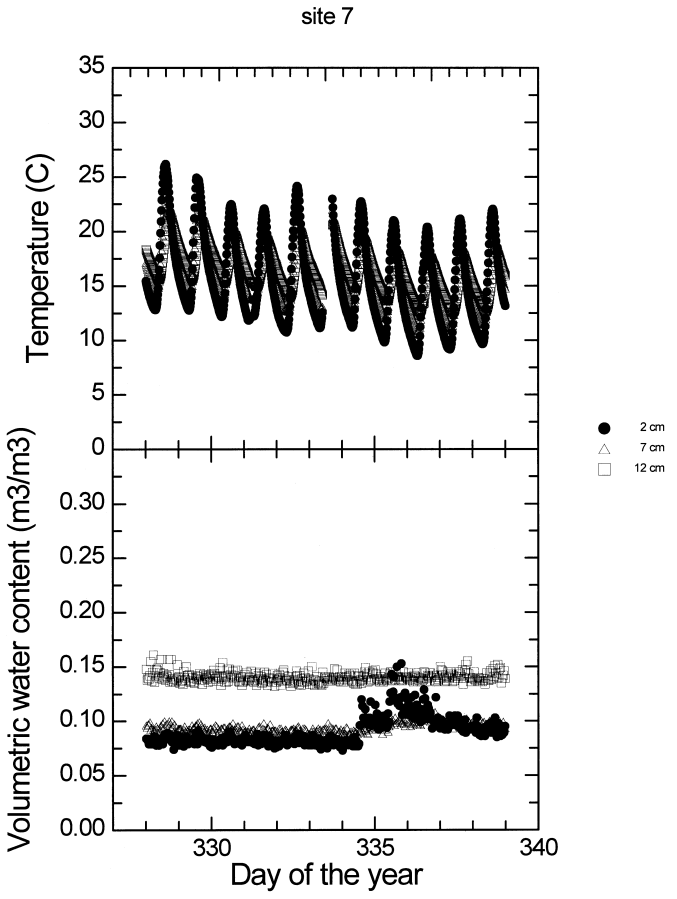

Fig. 4. Temporal variability of Θ and T at different depths at site 7 across days 328–338. Irrigation was applied on day 334 (hr 10∼12 noon) and on day 335 (hr 9∼10 am).

3.2. Temporal distribution of Θ and T

The temporal dynamics of T and Θ across days 328 through 338 at three typical sites are presented in Figs. 4–6. The T data show typical sinusoidal diurnal behavior at all three depths. The amplitude of the diurnal cycle, however, varied from site to site, depth to depth, and day to day. Water input (irrigation) on day 334 did not seem to have a significant impact on the amplitude of T at any site. In general T showed a seasonally decreasing trend versus time. Unlike T, the Θ data did not reveal any clear diurnal structure except for minor fluctuations across a day. Irrigation on day 334 caused a significant increase in Θ only at the 2 cm depth of all monitoring locations, whereas small or almost no changes in Θ were found at most 7 cm and 12 cm depths. Before irrigation on day 334, higher or lower values of $\Theta_{2\ \mathrm{cm}}$, as compared to $\Theta_{7\ \mathrm{cm}}$ and/or $\Theta_{12\ \mathrm{cm}}$, presumably reflected spatial variability in the soil hydraulic properties (and their temperature dependence) versus depth across the experimental field.

3.3. Spatio-temporal distribution of Θ and T

Figs. 7 and 8 show diurnal spatio-temporal variability of the soil water content and the soil temperature at two depths for days 328 through day 338. As in Mohanty et al. (1995), the spatial mean was plotted

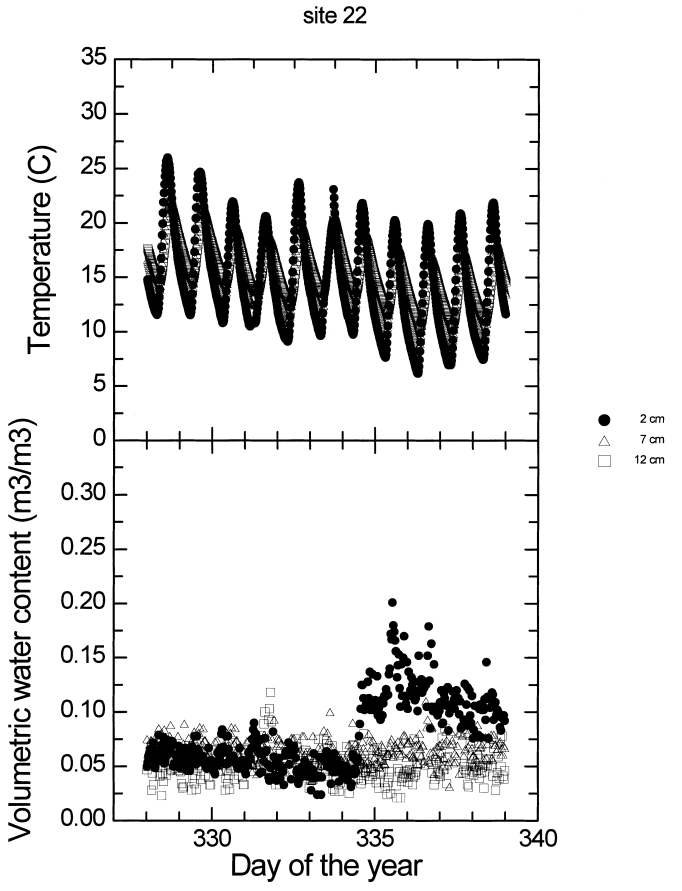

Fig. 5. Temporal variability of Θ and T at different depths at site 22 across days 328–338. Irrigation was applied on day 334 (hr 10∼12 noon) and on day 335 (hr 9∼10 am).

versus the variance in Θ or T at different times. Diurnal hysteretic loops in T similar to those in Mohanty et al. (1995) were found for all depths indicating differential soil heating and cooling sequences across the field. Lower loops corresponded to late night and early morning hours, whereas upper loops covered most parts of the day and the evening hours. These findings were confirmed by the phase lags in the diurnal temperature cycles at different locations in the field. An analysis of observed diurnal variations in atmospheric state variables revealed that the maximum (near-surface) air temperature and wind speed normally occur during 3:00∼4:00 pm, and coincide with the start of the cooling phase of the soil. We believe that interactive complex relationships between the spatial and temporal distribution of net radiation, air temperature, and near-surface wind speed are likely a reason of the observed spatio-temporal hysteresis in T. Presumably heating is largely due to the absorption of short-wave radiation which would be influenced by small variations in aspect (affect the incoming flux density) and surface roughness (affecting the albedo). While land surface was fairly flat, only microtopography might have any influence on soil thermal properties near the monitoring locations. In contrast, cooling will be largely due to long-wave emission, a process which spatially likely is much more uniform. As expected, the magnitude of the hysteretic variance

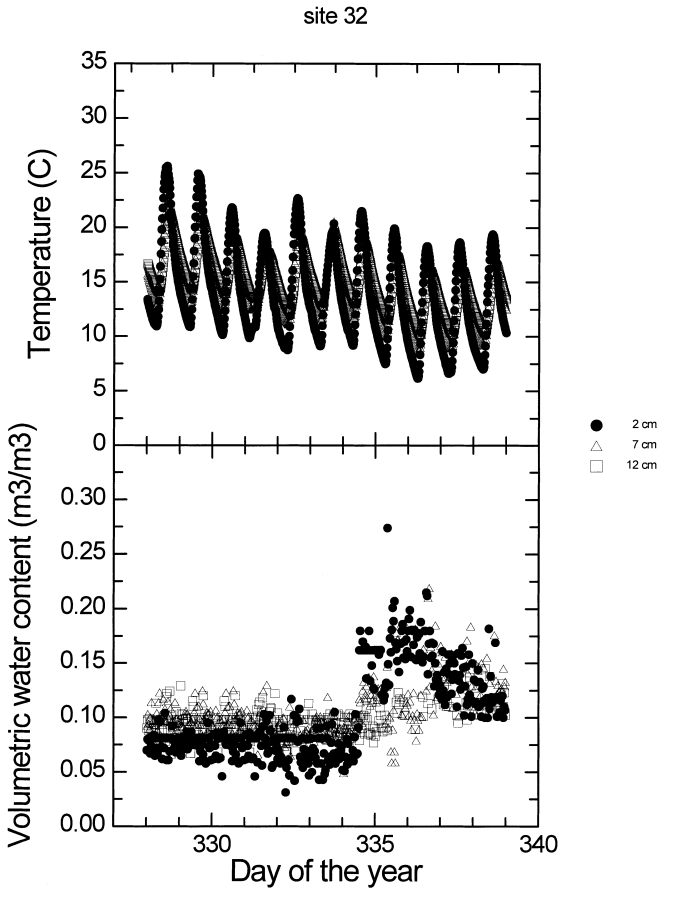

Fig. 6. Temporal variability of Θ and T at different depths at site 32 across days 328–338. Irrigation was applied on day 334 (hr 10∼12 noon) and on day 335 (hr 9∼10 am).

decreased with soil depth (Figs. 7 and 8). With increasing soil depth, the reduction in hysteresis of the lower loop is relatively smaller than the upper loop, thus leading to more symmetric plots. One interesting observation was that the diurnal hysteretic loops for T remained relatively small for several days following the irrigation events. One apparent reason for this behavior is the higher air/water ratio in the soil during dry days, which causes a higher variability in the thermal conductivity across the field, and hence in the soil temperature. The diurnal hysteretic behavior might ultimately be linked to surface fluxes of heat and water vapor. Although the exact reasons are still being studied, the fact that similar findings were obtained for different soil, tillage practice/microtopography and climatic conditions in Iowa (Mohanty et al., 1995) and California (this study) could indicate that the hysteretic phenomenon is a universal feature. The hysteresis may prove to be important when interpreting diurnal thermodynamics at different hydrologic scales.

A similar spatio-temporal analysis of corresponding Θ's at the same depths did not show any hysteresis across the day (Figs. 7 and 8). Rather, plots of the spatial mean and variance of the Θ data produced several clusters versus time in response to the irrigation event on day 334. In other words, the variance in Θ was relatively stationary across the mean for an individual cluster (or water regime) but nonstationary across different clusters (when the field was irrigated).

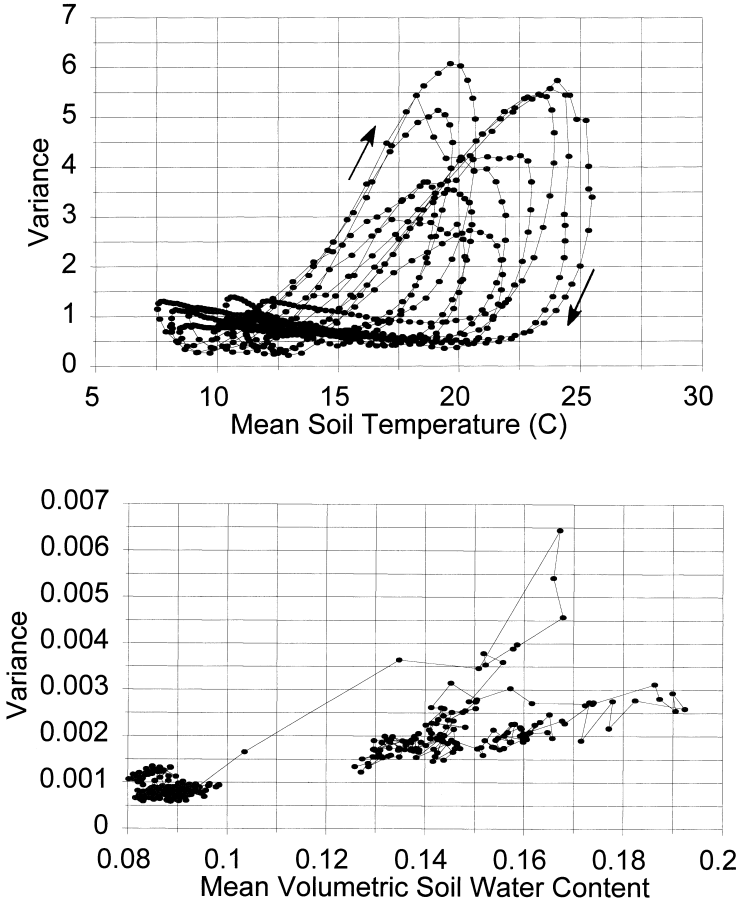

Fig. 7. Spatio-temporal variability of Θ and T at the depth of 2 cm. Mean and variance are calculated across all 49 monitoring locations (except occasional missing data).

These hysteretic or cluster type nonstationary spatio-temporal patterns in the T and Θ data warrant further research on adaptive data transformation and/or pre-processing (e.g., trend removal, median polishing) prior to any spatio-temporal or geostatistical analyses. In several follow-up papers we will address the spatio-temporal structures of T and Θ as well as their implications for field-scale heat and water transport modeling.

4. Conclusions

A field-scale study of water and heat flow was conducted in Riverside, California, using a space-extensive and time-intensive monitoring scheme. Soil water contents and soil temperatures were measured at 49 sampling locations and at three depths (2, 7, and 12 cm) using TDRs and thermocouples at 20 min intervals for 45 days under different soil moisture regimes. The experiment produced a unique and comprehensive data set useful for quantifying the spatio-temporal dynamics of Θ and T. The data presented here reveal several interesting features. Most interestingly, a spatio-temporal hysteresis was observed in soil temperature, while the soil water content exhibited a clustering behavior versus time because of irrigation.

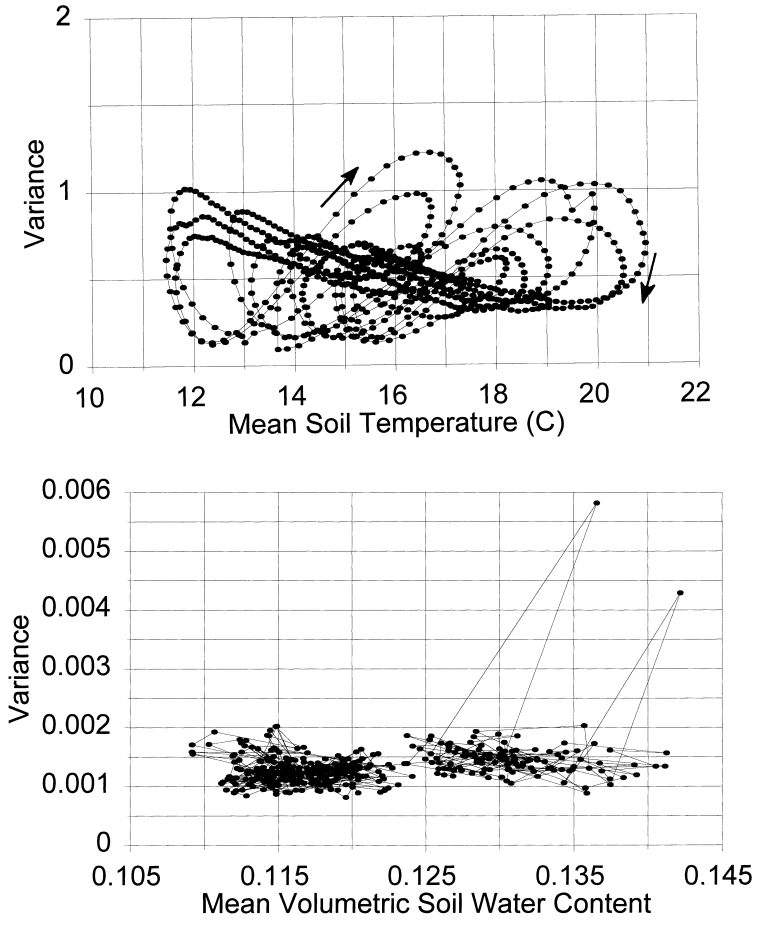

Fig. 8. Spatio-temporal variability of Θ and T at the depth of 12 cm. Mean and variance are calculated across all 49 monitoring locations (except occasional missing data).

References

Bell, K.R., Blanchard, B.J., Schmugge, T.J., Witczak, M.V., 1980. Analysis of surface moisture variations within large-field sites. Water Resour. Res. 16, 796–810.

Capehart, W.J., Carlson, T.N., 1997. Decoupling of surface and near-surface soil water content: A remote sensing perspective. Water Resour. Res. 33, 1383–1395.

Evett, S.R., Matthias, A.D., Warrick, A.W., 1994. Energy balance model of spatially variable evaporation from base soil. Soil Sci. Soc. Am. J. 58, 1604–1611.

Georgakakos, K.P., 1996. Soil moisture theories and observations, Special issue. J. of Hydrol. 184, 3–152.

Hills, R.G., Wierenga, P.J., Hudson, D.B., Kirkland, M.R., 1991. The second Las Cruces trench experiment: Experimental results and two-dimensional flow predictions. Water Resour. Res. 27, 2707–2718.

Jackson, T.J., Le Vine, D.M., Swift, C.T., Schmugge, T.J., Schiebe, F.R., 1995. Large area mapping of soil moisture using the ESTAR passive microwave radiometer in Washita'92. Remote Sens. Environ. 57, 27–37.

Jackson, T.J., 1997. Soil moisture estimation using special satellite microwave/imager satellite data over a grassland region. Water Resour. Res. 33, 1475–1484.

Mohanty, B.P., Klittich, W.M., Horton, R., van Genuchten, M.Th., 1995. Spatio-temporal variability of soil temperature within three land areas exposed to different tillage systems. Soil Sci. Soc. Am. J. 59, 752–759.

Mohanty, B.P., Bowman, R.S., Hendrickx, J.M.H., Van Genuchten, M.Th., 1997. New piecewise-continuous hydraulic functions for modeling preferential flow in an intermittent-flood-irrigated field. Water Resour. Res. 33, 2049–2063.

Noborio, K., McInnes, K.J., Heilman, J.L., 1996. Two dimensional model for water, heat, and solute transport in furrow-irrigated soil: II. Field evaluation. Soil Sci. Soc. Am. J. 60, 1010–1021.

Parlange, M.B., Katul, G.G., Nielsen, D.R., 1993. Determination of the field-scale diffusivity function, soil water storage, and evaporation. Water Resour. Res. 28, 2437–2446.

Radke, J.K., Reicosky, D.C., Voorhees, W.B., 1993. Laboratory simulation of temperature and hydraulic head variations under a soil ridge. Soil Sci. Soc. Am. J. 57, 652–660.

Shouse, P.J., Sisson, J.B., Ellsworth, T.R., Jobes, J.A., 1992. Estimating in situ unsaturated hydraulic properties of vertically heterogenous soils. Soil Sci. Soc. Am. J. 56, 1673–1679.

Shouse, P.J., Ellsworth, T.R., Jobes, J.A., 1994. Steady-state infiltration as a function of measurement scale. Soil Sci. 157, 129–136.

Staple, W.J., 1965. Moisture tension, diffusivity, and conductivity of a loam soil during wetting and drying. Can. J. Soil Sci. 45, 78–86.

Staple, W.J., 1969. Comparison off computed and measured moisture redistribution following infiltration. Can. J. Soil Sci. 33, 840–847.